Author/s:
Fuentes, S;Mahadevan, M;Bonada, M;Skewes, MA;Cox, JW

Title:
Night-time sap flow is parabolically linked to midday water potential for field-grown almond trees

Date:
2013-11-01

Citation:
Fuentes, S., Mahadevan, M., Bonada, M., Skewes, M. A. & Cox, J. W. (2013). Night-time sap flow is parabolically linked to midday water potential for field-grown almond trees. Irrigation Science, 31 (6), pp.1265-1276. https://doi.org/10.1007/s00271-013-0403-3.

# Night-time sap flow is parabolically linked to midday water potential for field grown almond trees.

Fuentes S.[a]*, Mahadevan M[b], Bonada M[a], Skewes M.A.[c] and Cox J.W. [a]

[a] University of Melbourne, Melbourne School of Land and Environment, VIC 3010, Australia

[b] South Australian Research and Development Institute. GPO Box 397. Adelaide, SA 5001. Australia

[C] South Australian Research and Development Institute, Loxton Research Centre, PO Box 411, Loxton, SA 5333, Australia

*Corresponding author: sfuentes@unimelb.edu.au

## ABSTRACT

To quantify night-time ($S_n$) and diurnal ($S_d$) tree water uptake, two sets of sap flow sensors (heat-pulse compensated) were installed per tree in the North-East and South-West sides of the trunk in three trees per treatment. There were two treatments: i) control, irrigated with 100% ETc ($T_{100}$) and ii) deficit, irrigated at 60% ETc ($T_{60}$) with daily irrigations at the peak atmospheric demand (Dec – Jan). Normalised $S_n$ by trees was in the range of 15 to 25% throughout the season, compared to normalised $S_d$, for $T_{100}$ and $T_{60}$ respectively. Furthermore $S_n$ was parabolically correlated to plant water status from the previous day, measured as midday stem water potential ($\Psi_s$). We also found strong correlations between $S_n$ and nocturnal VPD for $T_{100}$ and $T_{60}$, indicating that nocturnal transpiration ($E_n$) was significant for both treatments. Differences in $S_n$ were observed for the NE and SW sensors for $T_{60}$, being significantly less for the NE side (sunny side) compared to the SW side (more shaded). No differences were observed for $T_{100}$ regarding probe positioning.

**Keywords:** Night-time sap flow, midday stem water potential, night-time VPD, soil moisture.

## INTRODUCTION

Due to climate change predictions regarding reductions in rain events for most regions in Australia, there is a growing interest in the Australian Almond industry in increasing water use efficiency (WUE), especially in semi-arid regions, such as Berri (South Australia). One of the strategies considered to increase WUE is reducing water applied through regulated deficit irrigation (RDI), to achieve better stomata control through hormonal signals (mainly abscisic acid (ABA)) from roots to shoots. The hormonal effects of RDI in stomatal control and WUE have been widely studied for grapevines (Collins et al., 2009; Loveys et al., 2000; McCarthy et al., 2002; Rodrigues et al., 2008; Romero et al., 2012) and almonds (FuBeder et al., 1992; Wartinger et al., 1990). However, little attention has been given to nocturnal water uptake, and how much of this water corresponds to night-time transpiration ($E_n$).

It has been shown that the proportion of nocturnal sap flow to diurnal sap flow ($S_n/S_d$) can reach values up to 30 to 60% for arid and semi-arid regions in a range of ecosystems (Snyder et al., 2003). Furthermore, night-time water uptake does not always correspond to rehydration, and more often a significant part of $S_n$ has been ascribed to $E_n$ in a range of different species (Caird et al., 2007; Rogiers et al., 2009; Zeppel et al., 2010). Since $E_n$ is not associated with photosynthesis, it contributes toward decreased water use efficiency (WUE), which has a significant implication for the whole-tree water budget (Zeppel et al., 2010). When $E_n$ accounts for a high fraction of the $S_n/S_d$

proportion, $S_n$ is commonly highly correlated to nocturnal vapour pressure deficit (VPD) (Benyon, 1999; Fisher et al., 2007; Zeppel et al., 2010). Therefore, it is expected that $E_n$ would increase in a climate change scenario, which predicts that nocturnal temperatures will increase at a higher rate compared to diurnal temperatures (Brunetti et al., 2000; Easterling et al., 1997).

Since higher $E_n$ rates are expected with more soil moisture availability and higher night-time VPD, it will be difficult for plants to equilibrate their water status with that of the soil at night. For irrigation purposes, pre-dawn leaf water potential ($\Psi_{PD}$) has been commonly used to estimate plant water status under equilibrium conditions (Liang and Zhang, 1999; Remorini and Massai, 2003; Sousa et al., 2006). However, studies have already shown that this equilibrium between $\Psi_{PD}$ and soil water potential does not necessarily occur at night in a range of trees and shrubs (Bucci et al., 2005; Bucci et al., 2004; Donovan et al., 1999; Donovan et al., 2001; Sellin, 1999), and this lack of equilibrium has been associated with $E_n$ (Kavanagh et al., 2007). Therefore, it is important to characterise the proportion of $S_n/S_d$ through accurate quantification of these parameters to improve our understanding of the factors affecting $E_n$, and to obtain techniques to minimise this process.

Nocturnal water uptake and transpiration has been studied in a range of different species over the last 10 years (Caird et al., 2007), mostly trees (Kavanagh et al., 2007; Moore et al., 2008; Phillips et al., 2010; Wang et al., 2008; Zeppel et al., 2010), kiwifruit (Green et al., 1989) and grapevines (Flexas et al., 2002b; Rogiers et al., 2009). Until now, there has not been much literature available on night-time water uptake for Almond trees. This

study had as a general aim to contribute to the understanding of the dynamics of $S_n$ associated with plant water stress and atmospheric demand for irrigated almond trees grown in field conditions. Specific aims of this study were to compare $S_n$ and tree water stress, measured as midday stem water potential ($\Psi_s$) from the previous day and to explore the night-time capacity of almond trees to recover from water stress endured the previous day.

## MATERIALS AND METHODS

### *Field conditions and experimental details*

The experiment was conducted on 11-year-old almond trees [*Prunnus dulcis* (Mill.) Webb] at a commercial orchard (Clark Taylor farms) located in Berri, South Australia (34°20'S and 140°35'E) during the 2009 – 2010 season. The experimental site received an annual rainfall of 312mm in 87 rain days for the season (July 2009 to June 2010). Temperature ranged from -1.3°C in July to 44.3°C in January, with a maximum surface soil temperature of 49°C. There were two and six days with day-time temperature exceeding 40°C in December and January respectively. Weather conditions during summer (December, January and February) are presented in Table 1. The soil is classified as Sandy, uniform up to a depth of 150cm with a mean soil particle distribution of 89% sand, 2% silt, 9% clay, and a bulk density of 1.61 g $cm^{-3}$.

The almond orchard was planted in 1998 with the rows oriented roughly north–south. Trees were spaced 6.7m between rows and 6.1m within rows. The almond variety Nonpareil (50%), was considered for the experiment, these were inter-planted with Carmel (33%) in alternate rows and Ne Plus Ultra (17%) in every sixth row, both as pollinators. All trees were grafted on to

Nemaguard rootstock. Trees selected for the study had a trunk circumference of 90 to 100 cm at 30 cm from the ground, with a bark thickness of 5 to 8 mm.

*Irrigation and experimental design*

The orchard was drip irrigated. Each row of trees had two laterals, one on either side at 1 m offset from the tree trunk. The laterals had 4 L $h^{-1}$ pressure compensated button drippers spaced at 1 m interval. The laterals were buried at 10cm below ground level and water was delivered to the ground surface via a small tube attached to the outlet of each dripper. Each tree had approximately 12 drippers in total. Irrigation events occurred daily, commencing at 8 am with alternate on and off pulse cycles. The average flow rate of each dripper was 3.87 L $h^{-1}$.

Water for irrigation was pumped directly from the River Murray, with a separate water meter installed for each treatment to measure the volume of water applied. A Class-A evaporation pan was used to measure daily evaporation ($E_{pan}$) at the experimental site. Daily irrigation requirements (mm) were based on different crop factors according to the almonds' phenological stage. The crop factor (Kc) corresponding to this period from 11$^{th}$ December 2010 until the 1$^{st}$ of February 2010 was Kc = 1.0. After this date a change of Kc to 0.8 was implemented. This Kc change coincided with the final growth stage leading to harvesting. Further Kc changes were applied from the 12$^{th}$ of March (Kc = 0.7), 19$^{th}$ of March (Kc = 0.6) and 26$^{th}$ of March (Kc = 0.5). The crop factor (Kc) was multiplied by $E_{pan}$ to obtain crop evapotranspiration ($ET_c$). Rainfall was considered to be effective only when the total daily rainfall exceeded 12 mm.

The experiment consisted of five treatments with combinations of different fertilizer and water levels. Treatments were laid out in a randomised block design with three replications each. Treatment $T_{100}$ with 100% $ET_c$ irrigation and treatment $T_{60}$ with 60 % $ET_c$ irrigation were selected for sap flow studies. Both these treatments received the same levels of fertilizers *viz*., 320:54:600 (N:P:K) kg $ha^{-1}$ with the same fertilizer distribution pattern through the year, applied via fertigation.

*Sap flow measurements*

Three trees within each treatment were selected for sap flow measurements. Two sets of sensor probes were installed in each tree. The first probe for each tree was positioned on the North-East (NE) side of the tree and the second sensor on the South–West (SW) at around 50 cm above the ground surface. Sap flow measurements were performed using the heat pulse method as outlined (Green et al., 2003). The heat pulse velocity system used was based on the compensation method, with two temperature probes placed asymmetrically on either side (10 mm above and 5mm below) of the heater. The sensors and heater probes used for the study were purchased from TRANSFLO NZ LTD (Palmerston North, New Zealand)(Green, 1998). Stainless steel probes of 50mm length and 1.8mm thickness with four thermocouples at 5, 15, 25 and 40mm were used.

The sensors and heater probes were differentially wired to an AM25T multiplexer (Campbell Scientific Inc., Utah, USA). Heat pulses were automatically generated every 30 minutes using a CR1000 Campbell Scientific data logger (Campbell Scientific Inc., Utha, USA). Heat pulse

velocity was calculated according to the manufacturer specifications (Green, 1998). A correction factor for a 2.4mm wound width was used for calculations. The wood and sap fractions were 0.5 and 0.4 respectively. Volumetric sap flux was integrated over the sapwood area; taking into consideration the tree circumference, bark thickness and heartwood radius.

Night-time sap flow ($S_n$) was considered between 7 PM and 5 AM the next day (10 hours from sun-set to sun-rise). Sap flow for the period morning until midday ($S_{md}$) was considered from 5 AM until 3 PM (10 hours from sun-rise to end of measurements). Total day-time sap flow ($S_d$) was considered considering a 23.5 hour period (from 12:00 AM until 11:30PM).

Leaf area index (LAI) mas obtained the 1$^{st}$ of February 2010 using digital cover photography from trees in which sap flow probes were installed. Images were obtained just below the tree and in between of trees to calculate an averaged LAI (with a total of three images per tree). The digital images were analysed following the methodology proposed by Fuentes et al. (2008).

*Meteorological data*

Meteorological data for calculation of vapour pressure deficit (VPD) was obtained from the South Australian Murray-Darling Basin Natural Resource Management Board website (http://www.aws-samdbnrm.sa.gov.au). Data was collected from Bookpurnong (34$^o$21'S; 140$^o$36'E), the nearest meteorological station to the site,, located 200 m away from the trial site. .

*Soil moisture, soil physical and chemical properties*

Six Enviroscan® soil moisture probes (Sentek Pty. Ltd., Stepney, SA, Australia) where installed at 20 cm intervals laterally out from the drippers at distances between 0 and 100 cm. Each probe had five sensors at 20, 40, 60, 80 and 120 cm depths. All probes were wired to a RT6® data logger, and soil moisture data was recorded every hour.

Soil samples were obtained at similar depths to the soil moisture sensors (30, 60, 90, 150 cm), before installation of sap flow sensors. Soil textural properties were analysed separately for per cent of clay, silt and sand according to the procedure outlined by Day (1965). Salinity levels ($dsm^{-1}$) and organic matter (%) were determined using soil samples and laboratory analysis (Rayment and Higginson, 1992) (Table 2).

*Pre-dawn soil water potential calculations ($\Psi_{PDsoil}$)*

Pre-dawn soil water potential was calculated from soil moisture data obtained from the three probes (0, 20 and 40 cm) closest to the drippers. The conversion from volumetric soil moisture ($\theta_s$) to tension [$\Psi_{PDsoil}$ (MPa)] was made using the hydrological solutions approach (Saxton and Rawls, 2006; Saxton and Willey, 2004). The derived conversion equations were obtained using the SPAW hydrologic model (Saxton and Rawls, 2006; Saxton and Willey, 2004) and soil physical and chemical properties for each soil layer obtained from Table 2.

*Leaf ($\Psi_L$) and Stem ($\Psi_S$) water potential measurements*

Midday observations on leaf water and stem water potentials were carried out in parallel for the two treatments using Plant Water Status Console Apparatus, *Model 3000* (Soil Moisture Equipment Corporation Santa Barbara, CA, USA). Measurements were expressed in mega Pascals (MPa). Measurements were made on a weekly basis from the 1$^{st}$ of December 2009 until the 10$^{th}$ of February 2010. In total there were eight measurement dates for water potential (Table 3). The time of measurements was between 12:00 noon and 3:00 pm, which was regarded as "midday". Leaves for $\Psi_S$ were enclosed in a plastic bag coated with aluminium foil for a minimum of 10-15 minutes prior to measurement (Fulton et al., 2001).

Leaf water potential measurements ($\Psi_L$) were carried out on three fully expanded leaves per tree replicated three times for each treatment. The leaves selected were positioned in the top, middle and lower sections of tree canopies from the sunny side. All $\Psi_L$ measurements were performed within 30 s from leaf removal and expressed in MPa. Stem water potential ($\Psi_S$) measurements were carried out on one fully expanded leaf per tree replicated three times for each treatment.

*Zero-flow models*

A simple zero-flow model was proposed for each irrigation treatment. These zero-flow models were obtained by solving the equations obtained from the parabolic relationships comparing $S_n$ and $S_{md}$ with midday $\Psi_S$. The two solutions for each model (roots) were obtained using the "solver" function from MATLAB® R2011b (The Mathworks Inc., Natick, MA, USA).

*Data analysis*

To compare midday $\Psi_S$ with $S_n$ and $S_{md}$; $S_n$ with night-time VPD; midday $\Psi_S$ with $\Psi_L$; and $S_n/S_d$ proportion across treatments, general linear and curvilinear models were fitted to the data using MATLAB® R2011b (The Mathworks Inc., Natick, MA, USA) and the Curve Fitting Toolbox™. To evaluate the strength of relationships the standard error of estimates (SEE) and the root mean squared error (RMSE) were calculated. To explore whether specific treatments were uncoupled from the different relationships, a residual analysis with statistical significance was assessed using SigmaPlot® (Cranes software international Ltd, Bangalore. India) (Mayo et al., 2009; Monzon et al., 2006; Sadras and Moran, 2012; Tang et al., 2011).

Maximum, minimum and actual values of $S_n$ and $S_d$ per irrigation treatment were used to obtain the normalised ratio ($N(S_n/S_d)$) of sap flows using the following relationship:

Equation 1

where, $NS_{(n,d)}$ is the normalised value of $S_n$ or $S_d$; $Si_{(n,d)}$ is the actual value of $S_n$ or $S_d$; $S_{min}$ = the minimum flow of $S_n$ or $S_d$; $S_{max}$ = the maximum flow of the dataset.

## RESULTS

*Night-time dynamics of $S_n$ compared to available water and $S_d$*

The dynamics of $S_n$ was strongly influenced by the amount of water supplied by irrigation and rain events for both treatments ($T_{100}$ and $T_{60}$). Figure 1a shows total night-time water uptake by trees with their corresponding water inputs as irrigation and rain. The correlation between $S_n$ and water supply was closer during the early season period, which corresponded from the beginning of the study (24$^{th}$ November 2009) until the 2$^{nd}$ of February 2010. After this period, $S_n$ was lower in both irrigation treatments, right up to the end of the experimental period (24$^{th}$ March 2010) (regarded as late season period).

Figure 1b shows the $S_n$ trends compared to $\Psi_{PDsoil}$ (MPa) calculated at 5 am from soil moisture measurements. There was an apparent inverse relationship between $S_n$ and $\Psi_{PDsoil}$, which was more evident in $T_{60}$, especially for the early season period (until the 2$^{nd}$ of February 2010). From the 2$^{nd}$ of February to the 4$^{th}$ of March 2010, this relationship was maintained even though there was more water available in the soil through rain and irrigation. From the 4$^{th}$ of March until the end of the season the soil was close to field capacity. Non water-stressed conditions are marked with a horizontal dashed line passing through -0.5 MPa for $\Psi_{PDsoil}$ (Romero et al., 2004).

Values of $S_n$ were consistently higher for $T_{100}$ compared to $T_{60}$ throughout the whole season, with the exception of the first and last week of the period shown in Figure 1a and 1b. The average seasonal reduction of $S_n$ for $T_{60}$ compared to $T_{100}$ was 21%, with a maximum of 39% and a minimum of 3%.

Table 4 shows the total water applied (TWA) for the whole season (including irrigation and rain). Only 45% of the TWA was accounted for as diurnal sap flow ($S_d$) for $T_{100}$ and 55% for. From this total sap flow, 20% corresponded to $S_n$ for both treatments.

The normalised proportion comparing both irrigation treatments is shown in Figure 2, minimum and maximum values of this relationship corresponded to between 15 - 25% respectively from the $S_n/S_d$ relationship throughout the entire study period (early season and late season) for both treatments. Specifically, these $S_n/S_d$ percentages corresponded to minimum flows of around $S_n$ = 8 L tree$^{-1}$ night$^{-1}$ and $S_d$ = 52 L tree$^{-1}$ day$^{-1}$ and maximum flows of $S_n$ = 55 L tree$^{-1}$ night$^{-1}$ and $S_d$ = 218 L tree$^{-1}$ day$^{-1}$ for both treatments in average. In general, as shown in Fig. 2, the $N(S_n/S_d)$ proportion was similar for $T_{100}$ compared to $T_{60}$ as demonstrated by a high and statistically significant correlation ($R^2$ = 0.71; SEE = 0.054; RMSE = 0.017; $P < 0.05$) with slope close to unity (b = 0.86).

*Relationship between $S_n$ and midday $\Psi_S$*

Significant parabolic relationships were found when comparing $S_n$ with midday $\Psi_S$ measured the previous day for both treatments (Figure 3a; Table 5) for the measurement days (Table 3). These relationships were found for the early season period described, which ended the 2$^{nd}$ of February 2012. Two sections were identified for each parabolic relationship: i) the first section corresponded to $\Psi_S$ values from close to zero down to the peak of $S_n$ for each parabola (Table 5); ii) the second section corresponded to values of $\Psi_S$ to the left of peak $S_n$. Data from $T_{100}$ fell entirely within the first section described above. A

semi-parabola was found for $T_{100}$ and a more complete parabola was found for $T_{60}$ (Table 5). Statistical analysis of residuals showed that the treatments were uncoupled from each other for the $\Psi_S$ versus $S_n$ relationship ($P < 0.0006$) (Figure 3a). Results of the $\Psi_S$ *versus* $S_n$ relationship for different probe locations and treatments are shown in Figure 3b. Statistical analysis showed that the residuals for $T_{100}$NE, $T_{100}$SW and $T_{60}$SW were not statistically different for the first section of the parabola. By contrast, residuals from $T_{60}$NE were statistically different from both $T_{100}$ probe locations and the $T_{60}$SW ($P < 0.0001$). Data from $T_{60}$NE corresponded to a reduction of up to 31% from maximum values found in $T_{60}$SW and $T_{100}$ (Table 5).

*Relationship between $S_n$ and night-time VPD*

Statistically significant linear correlations ($P < 0.05$) were observed when comparing $S_n$ with night-time VPD (Table 6). The correlations were different during the two periods identified in Figure 1a. Hence, Figure 4a shows the $S_n$ *vs* night time VPD relationship from the early season period. Figure 4b shows the $S_n$ *vs* night time VPD relationship for the late season period. There was consistently higher $S_n$ in $T_{100}$ compared to $T_{60}$ for the same night-time VPD conditions during the early season period (Figure 4a), assessed by analysis of residuals ($P < 0.001$). There was less difference between $T_{100}$ and $T_{60}$ in the late season period (Figure 4b), however the $S_n$ *vs* VPD relationships of both treatments were also statistically significant and uncoupled, as assessed by analysis of residuals ($P < 0.001$).

*Relationship between $S_{md}$ and midday $\Psi_S$*

Significant parabolic relationships were obtained when comparing $S_{md}$ with midday $\Psi_S$ for both treatments (Figure 5 ; Table 5), which were similar to the results of $S_n$ and $\Psi_S$ for measurement dates (Table 3). Again, two sections were identified for each parabolic relationship. Data from $T_{100}$ and $T_{60}$ fell only in the first section and peak of a semi-parabola (Table 5).

Statistical analysis showed that the residuals for $T_{100}$NE and $T_{100}$SW were not statistically different (Figure 5, inset a). By contrast, residuals from $T_{60}$NE were statistically different from $T_{60}$SW ($P < 0.001$) (Figure 5, inset b). The calculated curve for $T_{60}$NE corresponded to a reduction of 26% from maximum values of $T_{60}$SW, and a 40% reduction from $T_{100}$ (Table 5).

## DISCUSSION

*Night-time water uptake ($S_n$) responds to soil water availability*

As demonstrated in Figure 1a, $S_n$ closely follows water input throughout the study period for both treatments. Therefore, it can be said that $S_n$ is a sensitive representation of tree water uptake at night-time, and that this will depend on the water availability within the soil surrounding the root-system, supplied mainly by irrigation and rain. The two main periods identified within the study season corresponded to the early season, characterised by more variable $S_n$ and water availability due to irrigation, rain and active diurnal and nocturnal water uptake. This period corresponds to the phenological stage of pit hardening and nut development followed by hull splitting in almond trees in the region. Two other factors might have contributed to reductions in $S_n$ for both treatments: i) a heavy rain event and strong winds on the 2$^{nd}$ of February

2010 (Figure 1a), which coincided with the onset of leaf senescence, and ii) incidence of leaf rust (*Tranzschelia discolour*) in that season following the rain. The combined effect of phenological stage of trees and the latter effects could explain the apparent non-responsiveness of $S_n$ to higher water availability by irrigation and rain for the late season period. Higher soil moisture (close to field capacity) and low water uptake by trees from both treatments demonstrates that there were over irrigations in the late season period. Therefore, the use of Kc for this period did not accurately reflect plant water use.

Furthermore, $S_n$ trends inversely responded to $\Psi_{PDsoil}$ for the early season period, as shown in Figure 1b. Therefore, $S_n$ is directly correlated to soil water availability, which is consistent with data presented in Fig 3a for the first section of the parabolic curve. Higher $S_n$ values for both treatments were associated with more negative $\Psi_{PDsoil}$ and *vice versa* and were associated to higher $\Psi_s$ values at midday. The $\Psi_{PDsoil}$ for T100 showed that trees on this irrigation treatment were maintained without water stress after irrigation events ($\Psi_{PDsoil}$ > -0.5) (Romero et al., 2004). By contrast, $T_{60}$ was maintained below this threshold for the early season period.

*Similar proportions of $S_n$ over $S_d$ found for $T_{100}$ and $T_{60}$*

The normalised $S_n/S_d$ proportion for both treatments corresponded to 15 to 25% (Figure 2), which falls in the lower range reported for trees in semi-arid regions (Snyder et al., 2003). A recent work found values of 6-8% on average for the season, with maximum values of 19% for a woodland area located in Richmond NSW (Temperate climate), which was ascribed mainly to $E_n$ (Zeppel et al., 2010).

*Night-time parabolic relationship between $S_n$ and midday $\Psi_S$*

Semi-parabolic relationships found for $T_{100}$ (Figure 3a) can be explained by the lack of stress in this treatment ($0 < \Psi_S < -1.2$ MPa) in all measurement dates (Table 3), which corresponded to the early season period analysed. Therefore, there is not sufficient data for $T_{100}$ to characterise the $S_n$ behaviour for lower $\Psi_S$ values. However, in preliminary data obtained in different grapevine varieties under initial no water-stress situations, followed by progressively greater water stress (Fuentes et al, unpublished) a complete parabolic relationship was found.

From the full parabolic relationship found in $T_{60}$, two stages were identified. The first section was characterised by higher $\Psi_S$ values (closer to zero), which corresponded to high water availability in the soil for both treatments for the corresponding measurement days (Table 3; Figure 1b), and low atmospheric demand at night-time for these dates (data not shown). Once that soil moisture started to deplete, $S_n$ increased up to a maximum (peak) value, which corresponded to mild water stress values of $\Psi_S$ for almond trees (Nortes et al., 2005; Shackel, 1995). This $S_n$ water flux may be associated

with increased $E_n$ and rehydration at night-time. The second stage of the parabolic curve was characterised by $\Psi_S$ values in the range associated with moderate to severe water stress in trees (Nortes et al., 2005; Shackel, 1995).

The $S_n$ versus $\Psi_S$ relationship was uncoupled for $T_{100}$ and $T_{60}$, as can be seen in Figure 3a, and through residual analysis. However, the main contributor to this decoupling between irrigation treatments is the NE (sunny side) of the $T_{60}$ treatment (Figure 3b). For stage 1 of the parabolic curves, there were no statistically significant differences between $T_{100}$ and $T_{60}$SW. This evidence supports the idea that the NE side of trees were submitted to higher stress compared to the SW side, the latter behaving at night-time as the $T_{100}$ treatment during stage 1 of the parabolic curves. Furthermore, it is a clear indication that single sap flow probes installed on large trees are not sufficient to assess accurately whole tree water uptake for both daytime (Figure 5b) and night-time (Figure 3b) flows, specially under mild to moderate water stress conditions.

The relationship between $S_n$ and $\Psi_S$ for higher $\Psi_S$ values (first part of parabola) might reflect the sensitivity of nocturnal stomatal conductance ($g_{night}$) to decreased soil water availability for stage 1 of the parabolic relationship, which is expected to be more evident during day-time, as shown in Figure 5a and 5b, where $T_{60}$ reduced daily maximum transpiration rate down to 32% of that recorded in $T_{100}$. Similar results were found for grapevines cv. Shiraz in Australia (Collins et al., 2009) and seven grapevine varieties in Mallorca (Spain) (Escalona et al., 2012). Figure 5b shows that significant differences were also found for day-time data between $T_{60}$SW and $T_{60}$NE, following the same pattern as night-time data for the measurement

days (Table 3).

Split root system experiments in tomato plants have demonstrated that under reduced water supply, ABA was also produced in leaves (Dodd, 2007; Dodd et al., 2008a; Dodd et al., 2008b). Furthermore, it is expected that the sunny side (NE) of trees under high VPD conditions will have a higher leaf synthesis of ABA (Davies et al., 2002; Wilkinson and Davies, 2002; Zhang and Zhang, 1994). Therefore, reduced water application and high sun exposure to a reduced leaf area index (from LAI in $T_{100}$ = $2.24^{a}$ to LAI in $T_{60}$ = $1.89^{b}$; $P < 0.05$) for $T_{60}$NE side of trees could explain reduced $S_{md}$ and $S_n$ for $T_{60}$ compared to $T_{100}$. According to these results, is possible that $T_{100}$ will be more affected by disequilibrium between pre dawn water potential and soil water content due to higher $S_n$, which may be associated to higher $E_{night}$ compared to $T_{60}$.

*Night-time atmospheric demand (VPD) as main driver of $S_n$*

Nocturnal sap flow ($S_n$) has been shown to contribute towards both nocturnal rehydration and $E_n$ (Snyder et al., 2003; Zeppel et al., 2010). Even though in this study we cannot possibly discriminate between night-time rehydration and $E_n$ from $S_n$ data, high correlations found between $S_n$ and night-time VPD (Figure 4a and 4b) for the early season period analysed suggest that $E_n$ could be the main component of this balance. This higher proportion of $E_n$ and high correlations with VPD has been previously showed for other tree species (Daley and Phillips, 2006; Kavanagh et al., 2007; Oren et al., 1999; Phillips et al., 2010; Zeppel et al., 2010), kiwifruits (Green et al., 1989) and grapevines (Fuentes et al., unpublished). A third component to account for in the $S_n$ balance is cuticular transpiration ($C_n$). However, it has been demonstrated that this component is minimal compared to $E_n$ and rehydration for trees (Zeppel et al., 2010) and grapevines (Flexas et al., 2002a).

According to Figure 1a, $S_n$ for both treatments increased as water availability within the rootzone increased. Since there were high and significant correlations between $S_n$ and VPD at night-time, it can be said that the same dynamics are expected for $E_n$. This is supported by observations of other tree species (Donovan et al., 2003; Zeppel et al., 2010)

*Night-time recovery capacity of trees from water stress endured the previous day*

Pre-dawn water potential ($\Psi_{PD}$) has been commonly used in almond trees to assess tree water status (Stevens et al., 2012). This has been based on the assumption that at night-time (pre-dawn) the $\Psi_{PD}$ will equilibrate with that of

the soil at zero-flow. However, there is evidence that this equilibrium is not met at night-time for a number of species, especially when trickle irrigation is used, which increases heterogeneity of wetting patterns within the rootzone (Bucci et al., 2005; Bucci et al., 2004; Donovan et al., 1999; Donovan et al., 2003; Donovan et al., 2001; Egea et al., 2011; Kavanagh et al., 2007; Sellin, 1999; Zeppel et al., 2010). By suggesting that an important proportion of $S_n$ corresponds to $E_n$, it is clear that the above assumption is not valid for our study in almond trees. Furthermore, the proportion of $S_n/S_d$ demonstrated a wide range, reaching values up to 25%, with an associated maximum value of $S_d$ = 62.4 L tree$^{-1}$ day$^{-1}$ and $S_d$ = 48.5 L tree$^{-1}$ day$^{-1}$ for $T_{100}$ and $T_{60}$ respectively, indicating for the latter case that more likely there is disequilibrium of $\Psi_{PD}$ is large in these situations. These large $S_n/S_d$ proportions may be used to more accurately estimate root surface water potentials and whole-tree hydraulic conductance (Zeppel et al., 2010). This disequilibrium also can be expected in the first stage, closer to the peak of the parabolic relationships between $S_n$ and $\Psi_{PD}$ according to data presented from the early season stage, which suggest that higher $S_n$, associated with higher $E_{night}$ is the main driver for higher $S_n/S_d$. Furthermore, the second stage found in the parabolic relationships between $S_n$ and $\Psi_{PD}$ is associated to lower capacity of trees to recover from stresses endured the day before, especially in $T_{60}$. The difficulties in recovery in stage 2 are also associated with reduced water availability in the soil, reduced tree hydraulic conductivity and shorter time period for recovery at night-time (summer period with shorter nights).

## CONCLUSIONS

Our study found that the proportion $S_n/S_d$ can reach values up to 25% for different irrigation treatments, and that $E_n$ might account for a large proportion of $S_n$ throughout the period of study. Differences in sap flow on different sides of the tree (exposed to sun and shade) are more evident in reduced water application treatments compared to control treatments. This effect needs to be taken into account when measuring $S_d$ and $S_n$ using sap flow probes, by installing at least two sets of probes per tree.

Two stages were apparent in the parabolic relationship between $S_n$ and midday $\Psi_S$. The results obtained in this study helped to support the hypothesis that stage 1 is characterised by the predominance of $E_n$ over rehydration due to more soil moisture availability and in stage 2 $E_n$ could be reduced due to reduced soil moisture available and less capacity to recover by the plant. Further research is required to separate the components of plant water uptake (rehydration, $E_n$ and $E_c$) to assess whether rehydration is maintained under mild to moderate water stress. This study supports the idea of developing this method further as a potential monitoring tool of the recovery capacity of plants from water stress.

**ACKNOWLEDGEMENTS**

We would like to acknowledge Almond Board of Australia, Berri, South Australia, for funding the project on “Minimising environmental foot prints from irrigated almonds by using new method and tools” of which the sap flow studies reported here were a part. We would also like to acknowledge Ben Brown and Brett Rosenzweig from the Almond Board of Australia for all their support and assistance for the experiment.

## TABLES

**Table 1:** Monthly average weather conditions at the experimental site during the early season period separated by day and night.

| Month | Temperature (°C) | | Relative humidity (%) | | Wind speed ($m\ s^{-1}$) | | Rainfall (mm) |
|---|---|---|---|---|---|---|---|
| | Day | Night | Day | Night | Day | Night | Total |
| December 2009 | 26 | 19 | 37 | 54 | 3.06 | 1.94 | 25 |
| January 2010 | 28 | 21 | 31 | 48 | 2.78 | 2.22 | 10 |
| February 2010 | 28 | 22 | 41 | 56 | 2.50 | 1.94 | 21 |

**Table 2:** Soil texture, organic matter and salinity at different depths for the experimental site.

| Treatment | Soil depth (cm) | Soil texture | | Organic Matter (%) Wt | Salinity dS $m^{-1}$ |
|---|---|---|---|---|---|
| | | Sand (%) | Clay (%) | | |
| $T_{100}$ | 30 | 90.2 | 9.8 | 0.50 | 2.02 |
| | 60 | 89.2 | 6.31 | 0.53 | 1.79 |
| | 90 | 87.2 | 6.10 | 0.17 | 1.26 |
| | 150 | 28.1 | 57.0 | 0.15 | 0.73 |
| $T_{60}$ | 30 | 92.1 | 5.9 | 0.69 | 2.41 |
| | 60 | 88.4 | 9.7 | 0.37 | 2.30 |
| | 90 | 90.2 | 9.8 | 0.16 | 1.50 |
| | 150 | 88.3 | 11.7 | 0.16 | 1.23 |

**Table 3:** Measurement dates for leaf ($\Psi_L$) and stem ($\Psi_S$) water potentials performed in both treatments ($T_{100}$ and $T_{60}$), showing average values obtained for each date corresponding to the early season.

| Date | Day of the year (DOI) | $T_{100}$ ($\Psi_S$; $\Psi_L$) MPa | $T_{60}$ ($\Psi_S$; $\Psi_L$) MPa |
|---|---|---|---|
| 1/12/2009 | 335 | -0.94; -1.42 | -1.04; -1.73 |
| 9/12/2009 | 343 | -0.62; -1.06 | -0.74; 1.26 |
| 22/12/2009 | 356 | -1.13; -1.88 | -1.38; 2.15 |
| 29/12/2009 | 363 | -1.25; -2.10 | -2.00; -2.21 |
| 6/01/2010 | 6 | -1.11; -1.59 | -1.21; -1.89 |
| 13/01/2010 | 13 | -0.76; -1.38 | -0.81; -1.17 |
| 20/01/2010 | 20 | -1.17; -1.96 | -1.61; -2.19 |
| 27/01/2010 | 27 | -0.82; -1.52 | -0.97; -1.55 |

**Table 4:** Comparison between total water applied for the whole studied season (TWA, includes irrigation and rain), irrigation only (I), diurnal sap flow ($S_n$), night-time sap flow ($S_n$) and water use efficiency (WUE) calculated by dividing total yield per treatment (data not shown) by total water applied.

| **Treatment** | **TWA** **ML ha$^{-1}$** | **I** **ML ha$^{-1}$** | **$S_d$** **ML ha$^{-1}$** | **$S_n$** **ML ha$^{-1}$** | **WUE** **kg ML$^{-1}$** |
|---|---|---|---|---|---|
| $T_{100}$ | 10.97 | 9.53 | 4.98 | 1.00 | 293 |
| $T_{60}$ | 7.26 | 5.82 | 4.02 | 0.80 | 374 |

**Table 5:** Statistical analysis of correlations and equations obtained for the relationships between $S_n$ (L tree$^{-1}$ night$^{-1}$); $S_{md}$ (L tree$^{-1}$) and $\Psi_S$ (MPa) for irrigation treatments and sap flow sensors orientation for the early season period.

| Treatment | Quadratic Equation ($S_n$ =)<br>Quadratic Equation ($S_{md}$ =) | SEE | $R^2$ | RMSE | Peak<br>($\Psi_S$; $S_n$)<br>($\Psi_S$; $S_{md}$) | Zero-flow night<br>Zero-flow day<br>(MPa) |
|---|---|---|---|---|---|---|
| $T_{100}$ | $-34.9 * \Psi_S^2 - 93.05 * \Psi_S - 21.67$<br>$-135.3 * \Psi_S^2 + 307.62 * \Psi_S - 52.14$ | 27.3<br>39.1 | 0.90*<br>0.96* | 2.61<br>4.42 | -1.34; 40.33<br>-1.14; 122.7 | -2.65ns; -0.26**<br>-2.09ns; -0.22** |
| $T_{60}$ | $-24.53 * \Psi_S^2 - 72.52 * \Psi_S - 20.3$<br>$-30.4 * \Psi_S^2 + 103.29 * \Psi_S + 0.46$ | 29.2<br>170 | 0.85*<br>0.82* | 2.70<br>5.83 | -1.48; 33.30<br>-1.70; 88.20 | -2.64*; -0.31**<br>-3.95ns; -0.37** |
| $T_{100}$ NE | $-30.9 * \Psi_S^2 - 83.76 * \Psi_S - 16.97$<br>$-191.4 * \Psi_S^2 + 413.6 * \Psi_S - 94$ | 42.7<br>15.8 | 0.84*<br>0.98* | 3.27<br>2.81 | -1.34; 39.78<br>-1.08; 129.4 | -2.50ns; -0.22**<br>-1.90ns; -0.26** |
| $T_{100}$ SW | $-38.95 * \Psi_S^2 - 102.4 * \Psi_S - 26.4$<br>$-135.3 * \Psi_S^2 + 307.62 * \Psi_S - 52.1$ | 34.3<br>39.13 | 0.89*<br>0.96* | 2.90<br>4.42 | -1.32; 40.90<br>-1.14; 122.8 | -2.34ns; -0.29**<br>-2.09*; -0.18** |
| $T_{60}$ NE | $-20.3 * \Psi_S^2 - 59.39 * \Psi_S - 15.68$<br>$-14.9 * \Psi_S^2 + 52.17 * \Psi_S + 28.5$ | 34.3<br>63.5 | 0.89*<br>0.80* | 2.90<br>3.25 | -1.46; 27.67<br>-1.76; 74.16 | -2.63*; -0.29**<br>-3.98ns; -0.48** |
| $T_{60}$ SW | $-28.7 * \Psi_S^2 - 85.70 * \Psi_S - 24.96$<br>$-22.7 * \Psi_S^2 + 83.8 * \Psi_S + 22.45$ | 41.6<br>7.22 | 0.85*<br>0.80* | 3.23<br>1.10 | -1.50; 38.95<br>-1.89; 99.79 | -2.66; -0.33**<br>-3.94*; -0.25** |

*Correlations are statistically significant at $P < 0.05$

** Zero-flow values were within 95% confidence bounds

ns non-significant.

**Table 6:** Statistical analysis of correlations and equations obtained for the relationship between $S_n$ (L tree$^{-1}$ night$^{-1}$) and night-time VPD (kPa) for the irrigation treatments during two periods; December-January (early season) and February-March (late season).

| Period | Treatment | Equation ($S_n$ =) | SEE | $R^2$ | RMSE |
|---|---|---|---|---|---|
| 1 | $T_{100}$ | 14.22 * VPD + 20.93 | 600 | 0.89* | 3.22 |
| | $T_{60}$ | 10.39 * VPD + 15.80 | 381 | 0.87* | 2.56 |
| 2 | $T_{100}$ | 10.11 * VPD + 7.41 | 1130 | 0.68* | 2.82 |
| | $T_{60}$ | 6.22 * VPD + 7.81 | 417 | 0.69* | 1.71 |

*Correlations are statistically significant at $P < 0.05$;

**Table 7:** Statistical analysis of correlations and equations obtained for the relationships between $S_n$ (L tree$^{-1}$ night$^{-1}$) and $\Psi_S$ (MPa) for irrigation treatments, and sap flow sensor orientation for $T_{60}$. Linear equations from non water-stressed $\Psi_S$ (MPa) values were used to obtain the diurnal and nocturnal behaviour in non-stressed situations for the early season.

| **Treatment** | **Linear Equation night ($S_n$ =)**<br>**Linear Equation day ($S_{md}$ =)** | **SEE** | **$R^2$** | **RMSE** |
|---|---|---|---|---|
| $T_{100}$ | $-27.33 * \Psi_S^2 + 7.65$ | 38.7 | 0.86* | 2.78 |
| | $57.5 * \Psi_S^2 + 56.2$ | 208 | 0.78* | 8.33 |
| $T_{60}$ | $-21.40 * \Psi_S + 5.10$ | 38.5 | 0.78* | 3.58 |
| | $23.62 * \Psi_S + 49.98$ | 52.2 | 0.88* | 2.95 |
| $T_{60}$ NE | $-11.8 * \Psi_S + 9.1$ | 25.5 | 0.71* | 2.91 |
| | $16.4 * \Psi_S + 48.5$ | 88.5 | 0.67* | 3.84 |
| $T_{60}$ SW | $-25.95 * \Psi_S + 4.70$ | 53.9 | 0.78* | 4.24 |
| | $30.8 * \Psi_S + 51.4$ | 36.9 | 0.95* | 2.48 |

*Correlations are statistically significant at $P < 0.05$.

## FIGURES

**Figure 1:** (a) Night-time dynamics of $S_n$ (L tree$^{-1}$ night$^{-1}$) for $T_{100}$ (black filled circles) and $T_{60}$ (open circles) in response to water application (rain and irrigation in m$^3$ tree$^{-1}$ day$^{-1}$) for an almond tree plantation (season 2009-10). Arrows indicate rain events; the length of the arrow is proportional to effective rain in L tree-1 associated with the $S_n$ scale. (b) Night-time dynamics of $S_n$ (L tree$^{-1}$ night$^{-1}$) for $T_{100}$ (black filled circles) and $T_{60}$ (open circles) in relation to $\Psi_{PDsoil}$ (MPa).

**Figure 2:** Relationship between the normalised $S_n/S_d$ proportion (N $S_n/S_d$) for $T_{100}$ compared to $T_{60}$ for the early season (black filled circles) and late season (grey filled circles).

**Figure 3:** (a) Parabolic relationships between midday $\Psi_S$ (MPa) and $S_n$ (L tree$^{-1}$ night$^{-1}$) for $T_{100}$ (black filled circles) and $T_{60}$ (grey filled circles) for measurement days throughout the early season. Residual analysis was performed to assess decoupling of treatments. (b) Parabolic relationships between midday $\Psi_S$ (MPa) and $S_n$ (L tree$^{-1}$ night$^{-1}$) by positioning of the probes within $T_{100}$ and $T_{60}$. Residual analysis was performed to assess decoupling of treatments and location of probes.

**Figure 4:** Relationship between night-time VPD (kPa) and $S_n$ (L tree$^{-1}$ night$^{-1}$) for $T_{100}$ (black circles) and $T_{60}$ (grey filled circles) for the early season period

(a); and the late season period (b). Residual analysis was performed to assess decoupling of treatments.

**Figure 5:** Parabolic relationships found between sap flow data measured from 5 AM until 2 PM ($S_{md}$ in L tree$^{-1}$)) and midday $\Psi_S$ (MPa) for $T_{100}$NE; $T_{100}$SW (black filled symbols) and $T_{60}$NE; $T_{60}$SW (grey filled circles). Residual analysis was performed to assess decoupling of treatments (insets a and b).

## REFERENCES


Benyon, R.G., 1999. Nighttime water use in an irrigated Eucalyptus grandis plantation. Tree Physiology, 19(13): 853-859.

Brunetti, M., Buffoni, L., Maugeri, M. and Nanni, T., 2000. Trends of Minimum and Maximum Daily Temperatures in Italy from 1865 to 1996. Theoretical and Applied Climatology, 66(1): 49-60.

Bucci, S.J. et al., 2005. Mechanisms contributing to seasonal homeostasis of minimum leaf water potential and predawn disequilibrium between soil and plant water potential in Neotropical savanna trees. Trees - Structure and Function, 19(3): 296-304.

Bucci, S.J. et al., 2004. Processes preventing nocturnal equilibration between leaf and soil water potential in tropical savanna woody species. Tree Physiology, 24(10): 1119-1127.

Caird, M.A., Richards, J.H. and Donovan, L.A., 2007. Nighttime Stomatal Conductance and Transpiration in C3 and C4 Plants. Plant Physiol., 143(1): 4-10.

Collins, M.J., Fuentes, S. and Barlow, E.W.R., 2009. Partial rootzone drying and deficit irrigation increase stomatal sensitivity to vapour pressure deficit in anisohydric grapevines. Functional Plant Biology, in press.

Daley, M.J. and Phillips, N.G., 2006. Interspecific variation in nighttime transpiration and stomatal conductance in a mixed New England deciduous forest. Tree Physiology, 26(4): 411-419.

Davies, W.J., Wilkinson, S. and Loveys, B., 2002. Stomatal control by chemical signalling and the exploitation of this mechanism to increase water use efficiency in agriculture. New Phytologist, 153(3): 449-460.

Dodd, I.C., 2007. Soil moisture heterogeneity during deficit irrigation alters root-to-shoot signalling of abscisic acid. Functional Plant Biology, 34(5): 439-448.

Dodd, I.C., Egea, G. and Davies, W.J., 2008a. Abscisic acid signalling when soil moisture is heterogeneous: decreased photoperiod sap flow from drying roots limits abscisic acid export to the shoots. Plant Cell and Environment, 31(9): 1263-1274.

Dodd, I.C., Egea, G. and Davies, W.J., 2008b. Accounting for sap flow from different parts of the root system improves the prediction of xylem ABA concentration in plants grown with heterogeneous soil moisture. Journal of Experimental Botany, 59(15): 4083-4093.

Donovan, L.A. et al., 1999. Predawn disequilibrium between plant and soil water potentials in two cold-desert shrubs. Oecologia, 120(2): 209-217.

Donovan, L.A., Richards, J.H. and Linton, M.J., 2003. Magnitud and mechanisms of desequilibrium between predawn plant and soil water potentials. Ecology, 84(2): 463-470.

Donovan, L.D., Linton, M.L. and Richards, J.R., 2001. Predawn plant water potential does not necessarily equilibrate with soil water potential under well-watered conditions. Oecologia, 129(3): 328-335.

Easterling, D.R. et al., 1997. Maximum and Minimum Temperature Trends for the Globe. Science, 277(5324): 364-367.

Egea, G., Dodd, I.C., González-Real, M.M., Domingo, R. and Baille, A., 2011. Partial rootzone drying improves almond tree leaf-level water use

efficiency and afternoon water status compared with regulated deficit irrigation. Functional Plant Biology, 38(5): 372-385.
Escalona, J. et al., 2012. Responses of leaf night respiration and transpiration to water stress in Vitis vinifera L. Agricultural Water Management, In press.
Fisher, J.B., Baldocchi, D.D., Misson, L., Dawson, T.E. and Goldstein, A.H., 2007. What the towers don't see at night: nocturnal sap flow in trees and shrubs at two AmeriFlux sites in California. Tree Physiology, 27(4): 597-610.
Flexas, J. et al., 2002a. Effects of drought on photosynthesis in grapevines under field conditions: an evaluation of stomatal and mesophyll limitations. Functional Plant Biology, 29(4): 461-471.
Flexas, J. et al., 2002b. Effects of drought on photosynthesis in grapevines under field conditions: an evaluation of stomatal and mesophyll limitations. Functional Plant Biology, 29(4): 461-471.
FuBeder, A., Wartinger, A., Hartung, W., Schulze, E.D. and Heilmeier, H., 1992. Cytokinins in the Xylem Sap of Desert-Grown Almond (Prunus dulcis) Trees: Daily Courses and Their Possible Interactions with Abscisic Acid and Leaf Conductance. New Phytologist, 122(1): 45-52.
Fulton, A. et al., 2001. Rapid equilibration of leaf and stem water potential under field conditions in almonds, walnuts and prunes. Hort Technology, 11(4): 609-614.
Green, S., 1998. Measurements of sap flow by the heat-pulse method. HortResearch, Palmerston North, New Zealand.
Green, S., Clothier, B. and Jardine, B., 2003. Theory and practical application of heat pulse to measure sap flow. Agronomy Journal, 95(6): 1371-1379.
Green, S.R., McNaughton, K.G. and Clothier, B.E., 1989. Observations of night-time water use in kiwifruit vines and apple trees. Agricultural and Forest Meteorology, 48(3&4): 251-261.
Kavanagh, K.L., Pangle, R. and Schotzko, A.D., 2007. Nocturnal transpiration causing disequilibrium between soil and stem predawn water potential in mixed conifer forests of Idaho. Tree Physiology, 27(4): 621-629.
Liang, J.S. and Zhang, J.H., 1999. The relations of stomatal closure and reopening to xylem ABA concentration and leaf water potential during soil drying and rewatering. Plant Growth Regulation, 29(1-2): 77-86.
Loveys, B.R., Dry, P.R., Stoll, M. and McCarthy, M.G., 2000. Using plant physiology to improve the water use efficiency of horticultural crops. Acta Horticulturae, 537(1): 187-197.
Mayo, N.E., Scott, S.C. and Ahmed, S., 2009. Case management poststroke did not induce response shift: the value of residuals. Journal of Clinical Epidemiology, 62(11): 1148-1156.
McCarthy, M.G., Loveys, B.R., Dry, P.R. and Stoll, M., 2002. Regulated deficit irrigation and partial rootzone dryig as irrigation management techniques for grapevines, FAO, Rome.
Monzon, J.P., Sadras, V.O. and Andrade, F.H., 2006. Fallow soil evaporation and water storage as affected by stubble in sub-humid (Argentina) and semi-arid (Australia) environments. Field Crops Research, 98(2&3): 83-90.

Moore, G.W., Cleverly, J.R. and Owens, M.K., 2008. Nocturnal transpiration in riparian Tamarix thickets authenticated by sap flux, eddy covariance and leaf gas exchange measurements. Tree Physiology, 28(4): 521-528.

Nortes, P.A., Perez-Pastor, A., Egea, G., Conejero, W. and Domingo, R., 2005. Comparison of changes in stem diameter and water potential values for detecting water stress in young almond trees. Agricultural Water Management, 77(1&3): 296-307.

Oren, R. et al., 1999. Survey and synthesis of intra- and inter-specific variation in stomatal sensitivity to vapour pressure deficit. Plant, Cell and Environment, 22(12): 1515-1526.

Phillips, N.G., Lewis, J.D., Logan, B.A. and Tissue, D.T., 2010. Inter- and intra-specific variation in nocturnal water transport in Eucalyptus. Tree Physiology, 30(5): 586-596.

Rayment, G.E. and Higginson, F.R., 1992. Australian laboratory handbook of soil and water chemical methods. Inkata Press, Melbourne, 330 pp.

Remorini, D. and Massai, R., 2003. Comparison of water status indicators for young peach trees. Irrigation Science, 22(1): 39-46.

Rodrigues, M.L. et al., 2008. Hydraulic and chemical signalling in the regulation of stomatal conductance and plant water use in field grapevines growing under deficit irrigation. Functional Plant Biology, 35(7): 565-579.

Rogiers, S.Y., Greer, D.H., Hutton, R.J. and Landsberg, J.J., 2009. Does night-time transpiration contribute to anisohydric behaviour in a Vitis vinifera cultivar? Journal of Experimental Botany, 60(13): 3751-3763.

Romero, P., Dodd, I.C. and Martinez-Cutillas, A., 2012. Contrasting physiological effects of partial root zone drying in field-grown grapevine (Vitis vinifera L. cv. Monastrell) according to total soil water availability. Journal of Experimental Botany, 63(11): 4071-4083.

Romero, P., Navarro, J.M., Garc√≠a, F. and Ordaz, P.B.a., 2004. Effects of regulated deficit irrigation during the pre-harvest period on gas exchange, leaf development and crop yield of mature almond trees. Tree Physiology, 24(3): 303-312.

Sadras, V.O. and Moran, M.A., 2012. Elevated temperature decouples anthocyanins and sugars in berries of Shiraz and Cabernet Franc. Australian Journal of Grape and Wine Research: no-no.

Saxton, K.E. and Rawls, W.J., 2006. Soil Water Characteristic Estimates by Texture and Organic Matter for Hydrologic Solutions. Soil Sci. Soc. Am. J., 70(5): 1569-1578.

Saxton, K.E. and Willey, P.H., 2004. Agricultural wetland and pond hydrologic analysis using SPAW model. ASAE.

Sellin, A., 1999. Does pre-dawn water potential reflect conditions of equilibrium in plant and soil water status? Acta Oecologica, 20(1): 51-59.

Shackel, K.A., 1995. Plant Water Status as an Index of Irrigation Needs in Deciduous Fruit Trees. Hortscience, 30(4): 905.

Snyder, K.A., Richards, J.H. and Donovan, L.A., 2003. Night‚Äêtime conductance in C3 and C4 species: do plants lose water at night? Journal of Experimental Botany, 54(383): 861-865.

Sousa, T.A., Oliveira, M.T. and Pereira, J.M., 2006. Physiological indicators of plant water status of irrigated and non-irrigated grapevines grown in a low rainfall area of portugal. Plant and Soil, 282(1-2): 127-134.

Stevens, R., Ewenz, C., Grigson, G. and Conner, S., 2012. Water use by an irrigated almond orchard. Irrigation Science, 30(3): 189-200.

Tang, K., Beaton, D.E., Gignac, M.A.M. and Bombardier, C., 2011. Rasch analysis informed modifications to the Work Instability Scale for Rheumatoid Arthritis for use in work-related upper limb disorders. Journal of Clinical Epidemiology, 64(11): 1242-1251.

Wang, H. et al., 2008. Nocturnal sap flow characteristics and stem water recharge of Acacia mangium. Frontiers of Forestry in China, 3(1): 72-78.

Wartinger, A., Heilmeier, H., Hartung, W. and Schulze, E.D., 1990. Daily and seasonal courses of leaf conductance and abscisic acid in the xylem sap of almond trees [Prunus dulcis (Miller) D. A. Webb] under desert conditions. New Phytologist, 116(4): 581-587.

Wilkinson, S. and Davies, W.J., 2002. ABA-based chemical signalling: the co-ordination of responses to stress in plants. Plant, Cell & Environment, 25(2): 195-210.

Zeppel, M., Tissue, D., Taylor, D., Macinnis-Ng, C. and Eamus, D., 2010. Rates of nocturnal transpiration in two evergreen temperate woodland species with differing water-use strategies. Tree Physiology, 30(8): 988-1000.

Zhang, J. and Zhang, X., 1994. Can early wilting of old leaves account for much of the ABA accumulation in flooded pea plants? Journal of Experimental Botany, 45(9): 1335-1342.

Fig. 1a

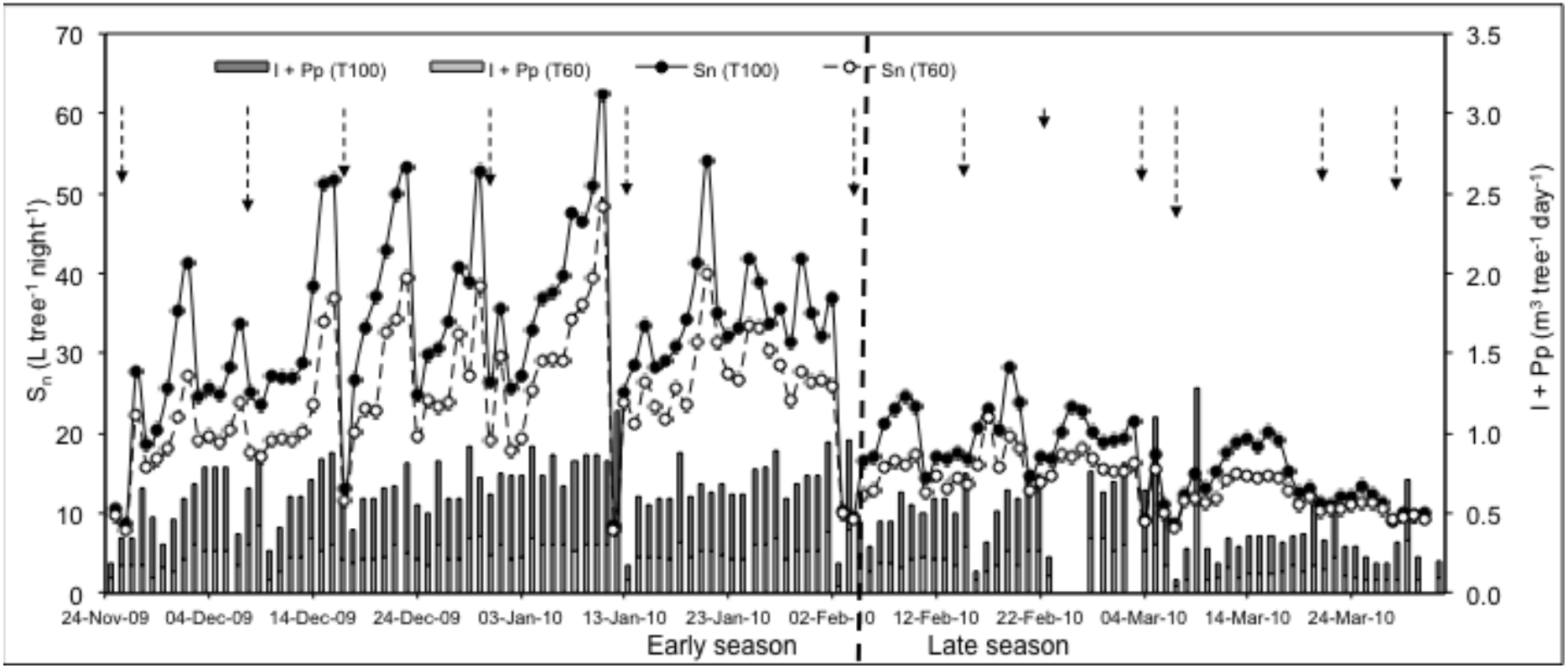
I + Pp (T100)
I + Pp (T60)
Sn (T100)
Sn (T60)
Sn (L tree-1 night-1)
I + Pp (m3 tree-1 day-1)
0
10
20
30
40
50
60
70
0.0
0.5
1.0
1.5
2.0
2.5
3.0
3.5
24-Nov-09
04-Dec-09
14-Dec-09
24-Dec-09
03-Jan-10
13-Jan-10
23-Jan-10
02-Feb-10
12-Feb-10
22-Feb-10
04-Mar-10
14-Mar-10
24-Mar-10
Early season
Late season

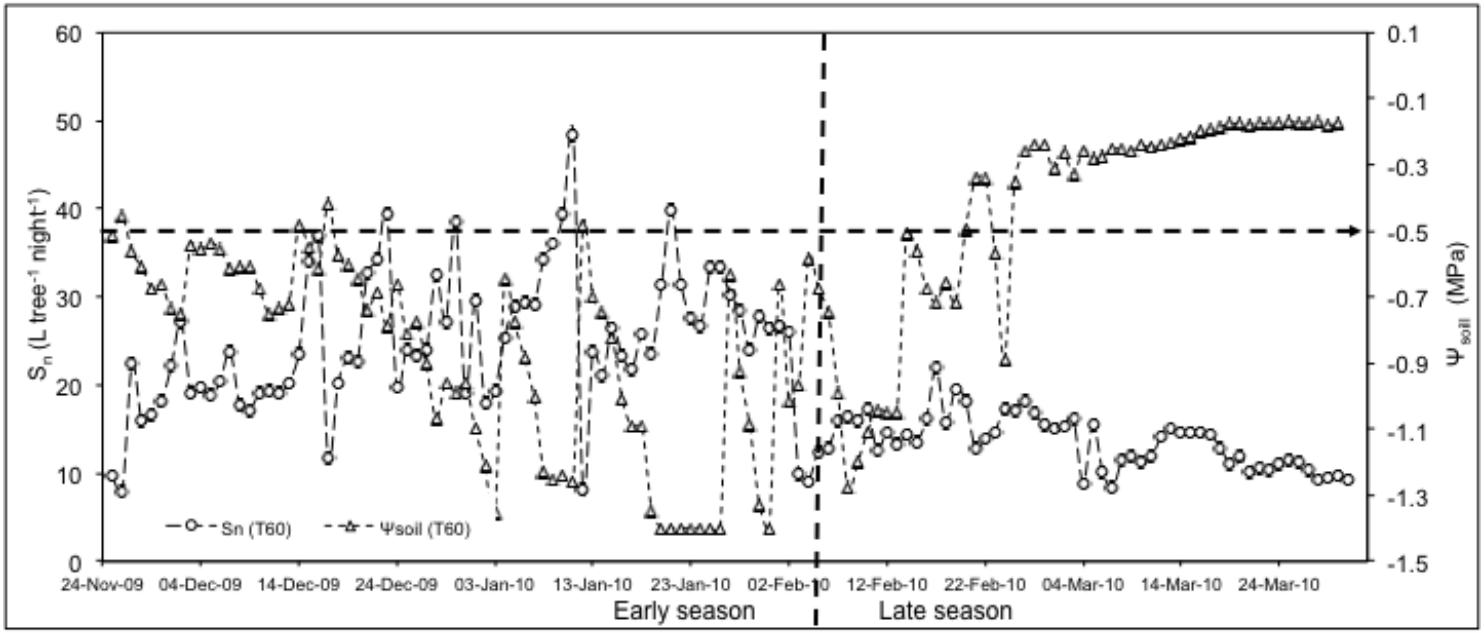
60
50
40
30
20
10
0
$S_n$ (L tree$^{-1}$ night$^{-1}$)
0.1
-0.1
-0.3
-0.5
-0.7
-0.9
-1.1
-1.3
-1.5
$\Psi_{soil}$ (MPa)
Sn (T60)
Ψsoil (T60)
24-Nov-09
04-Dec-09
14-Dec-09
24-Dec-09
03-Jan-10
13-Jan-10
23-Jan-10
02-Feb-10
12-Feb-10
22-Feb-10
04-Mar-10
14-Mar-10
24-Mar-10
Early season
Late season

Fig 1b

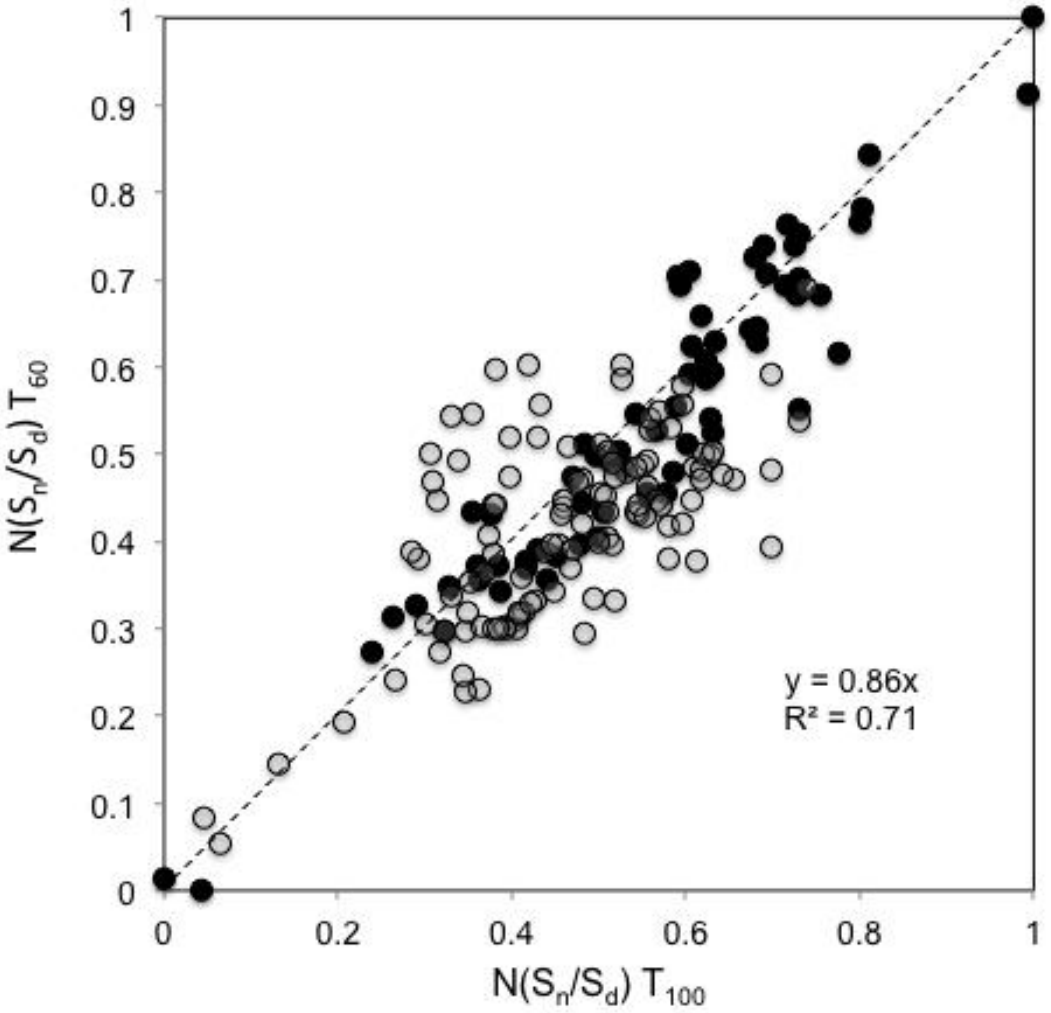
1
0.9
0.8
0.7
0.6
0.5
0.4
0.3
0.2
0.1
0
0
0.2
0.4
0.6
0.8
1
N(Sn/Sd) T60
N(Sn/Sd) T100
y = 0.86x
R² = 0.71

Fig. 2

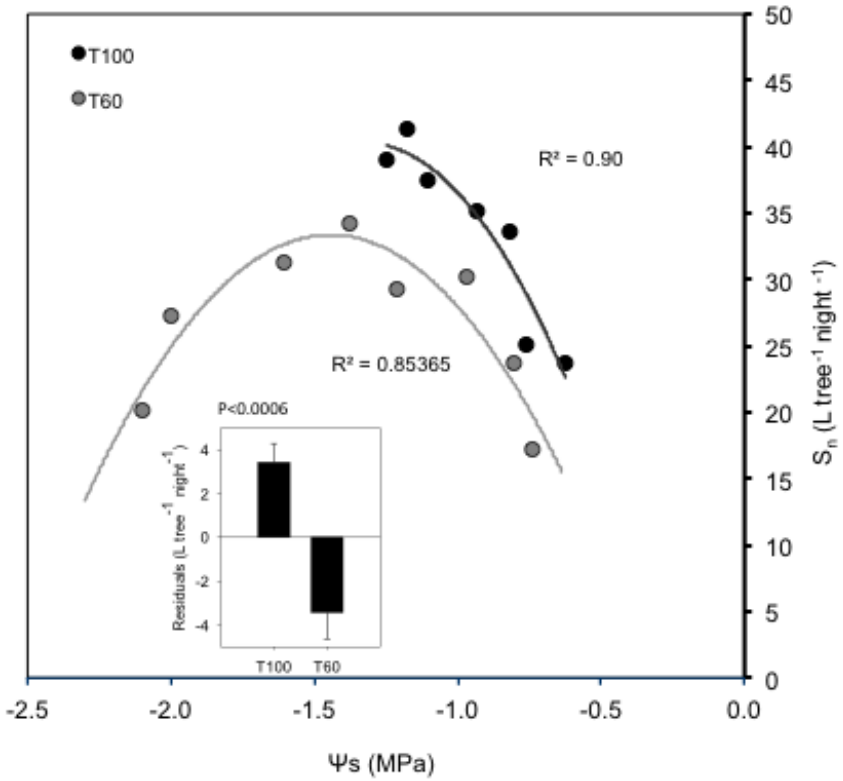
T100
T60
R² = 0.90
R² = 0.85365
P<0.0006
Residuals (L tree-1 night-1)
T100
T60
Ψs (MPa)
Sn (L tree-1 night-1)

Fig. 3a

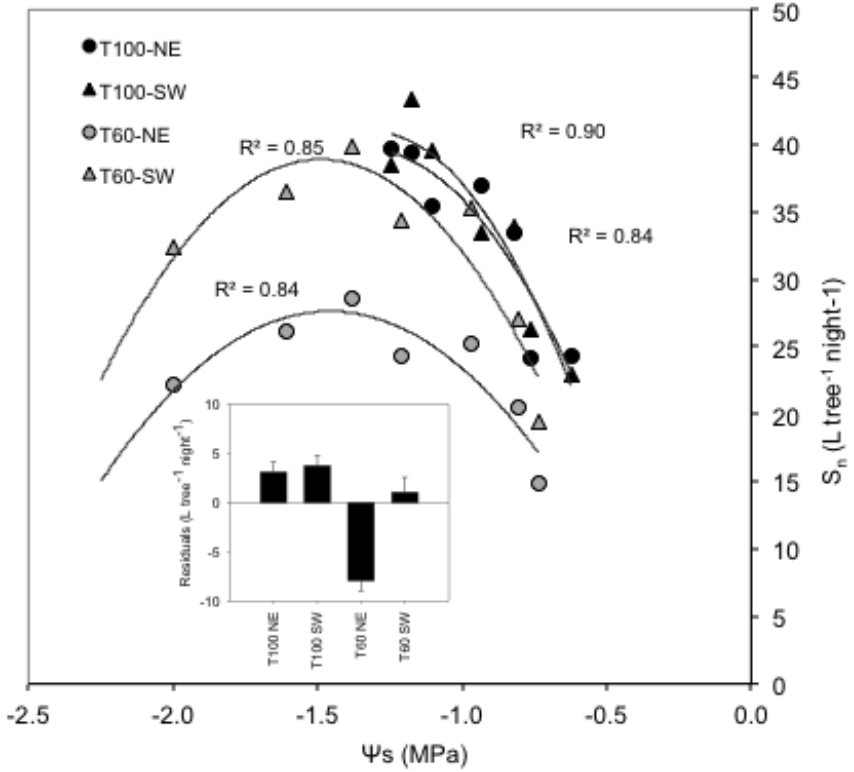
T100-NE
T100-SW
T60-NE
T60-SW
R² = 0.85
R² = 0.90
R² = 0.84
R² = 0.84
Residuals (L tree-1 night-1)
T100 NE
T100 SW
T60 NE
T80 SW
Ψs (MPa)
Sn (L tree-1 night-1)

Fig. 3b

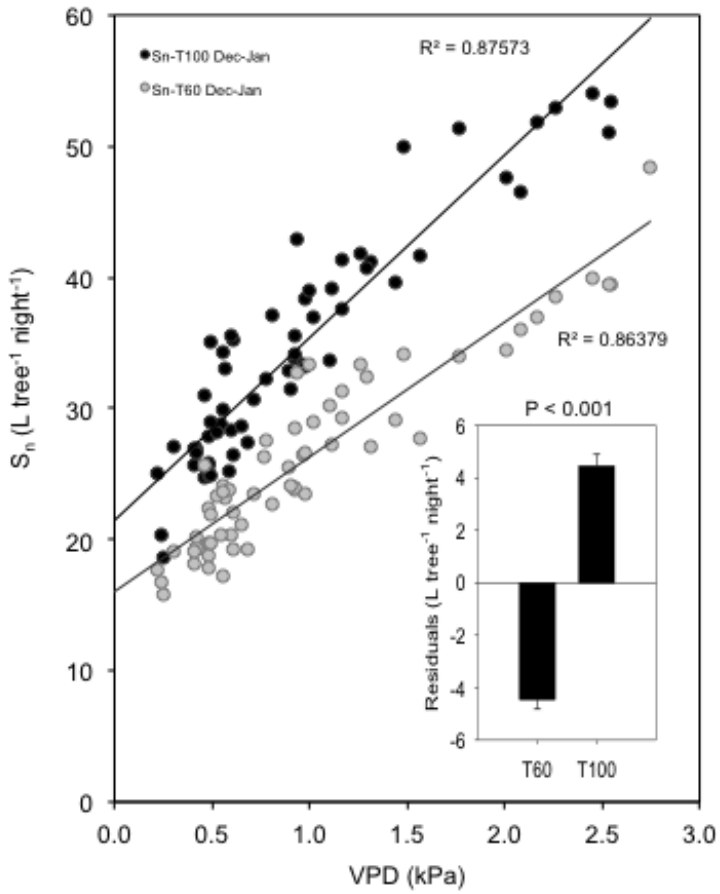
Sn-T100 Dec-Jan
Sn-T60 Dec-Jan
R² = 0.87573
R² = 0.86379
P < 0.001
Residuals (L tree⁻¹ night⁻¹)
T60
T100
Sn (L tree⁻¹ night⁻¹)
VPD (kPa)

Fig 4a

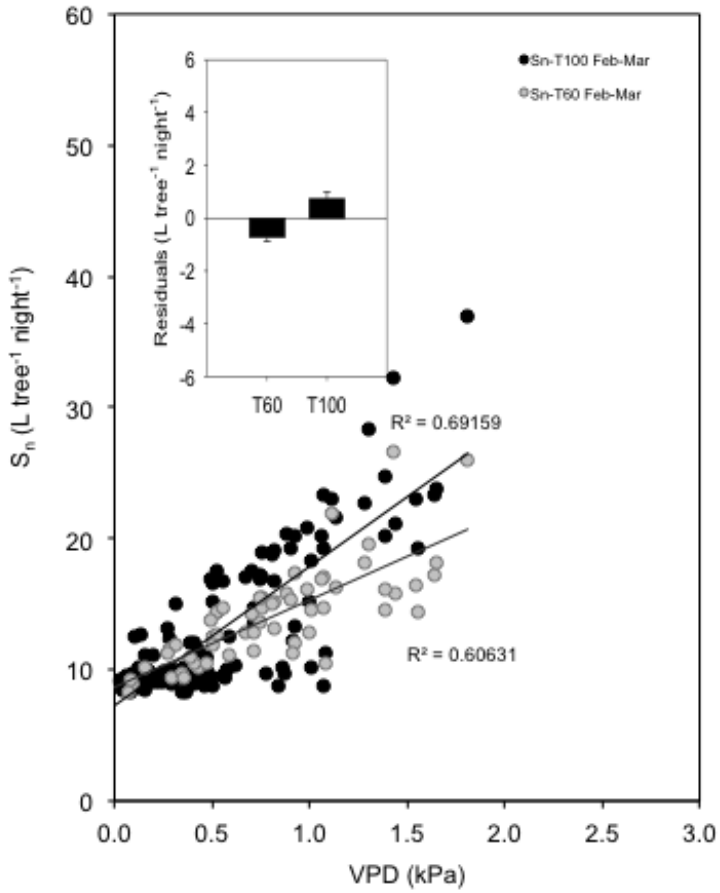
Sn-T100 Feb-Mar
Sn-T60 Feb-Mar
Residuals (L tree-1 night-1)
T60
T100
R² = 0.69159
R² = 0.60631
Sn (L tree-1 night-1)
VPD (kPa)

Fig 4b

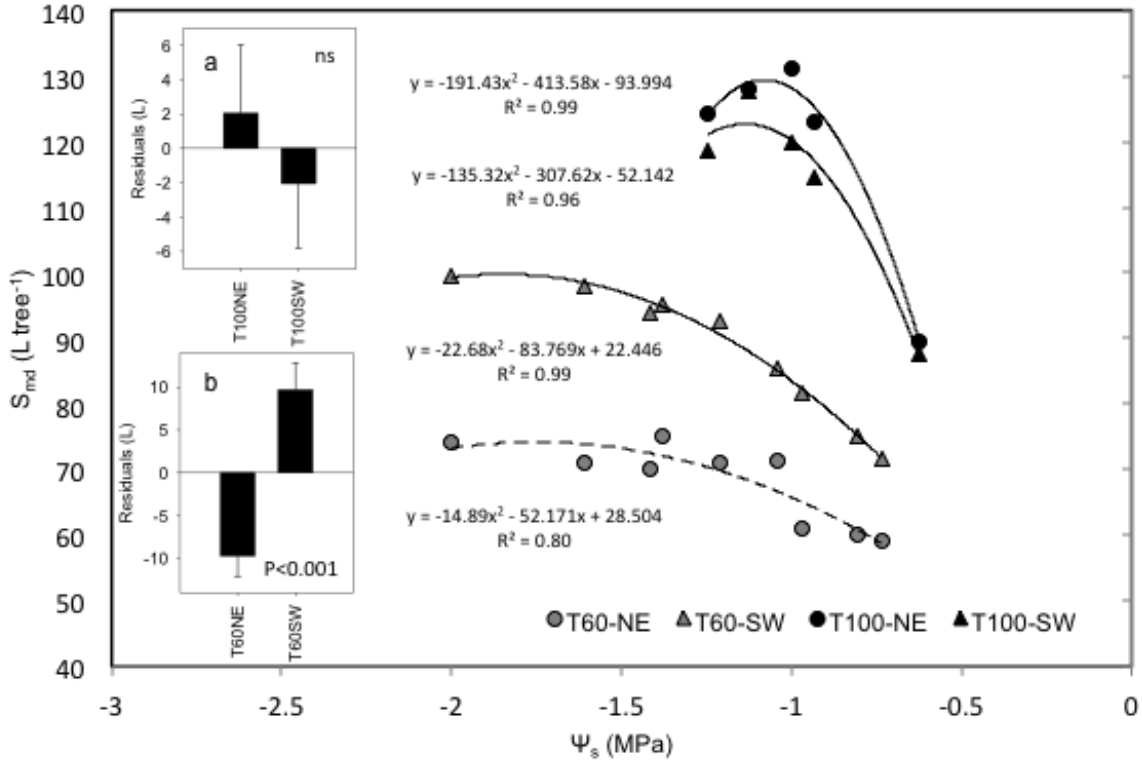
a
ns
Residuals (L)
T100NE
T100SW
b
P<0.001
T60NE
T60SW
y = -191.43x² - 413.58x - 93.994
R² = 0.99
y = -135.32x² - 307.62x - 52.142
R² = 0.96
y = -22.68x² - 83.769x + 22.446
R² = 0.99
y = -14.89x² - 52.171x + 28.504
R² = 0.80
T60-NE
T60-SW
T100-NE
T100-SW
S_md (L tree⁻¹)
Ψ_s (MPa)

Fig 5